

Synthesis of the four 1-(1-deoxy-D-pentitol-1-yl)thymines and conformational properties of the acyclic sugar chain

Scott M. Vejcik and Derek Horton*

Department of Chemistry, American University, 4400 Massachusetts Avenue, NW, Washington, DC 20016, USA

Received 23 October 2006; received in revised form 28 November 2006; accepted 5 December 2006

Available online 12 December 2006

Abstract—Acetylated D-pentose diethyl dithioacetals were coupled by way of 1-bromo-1-ethylthio derivatives with 2,4-bis(trimethylsilyl)thymine to afford diastereomeric pairs of acyclic-sugar nucleoside analogues bearing a thymine-1-yl and an ethylthio group at C-1. Free-radical desulfurization by the action of tributylstannane removed the ethylthio group to afford the corresponding acetylated 1-(1-deoxy-D-pentitol-1-yl)thymines and subsequently the free title compounds in the *arabino*, *lyxo*, *ribo*, and *xylo* series. Conformations of the intermediates and products were studied in detail and the final products were evaluated for their potential as agents active against plant viruses and rice blast fungus.

© 2006 Elsevier Ltd. All rights reserved.

Keywords: Nucleoside analogue; Acyclic sugar; Free-radical desulfurization; NMR spectroscopy; Chain conformation; Antifungal agent; Antiviral agent

1. Introduction

Nucleoside analogues in which the sugar component is in the open-chain form have been of sustained synthetic interest in this laboratory,^{1–4} as such products should in principle be inert to nuclease enzymes, could modify the solubility properties and transport behavior of the attached bases in biological systems, and might act as pro-drugs susceptible to phosphorylation by kinases, especially if the conformational disposition of the sugar chain would present a favorable orientation simulating a natural nucleoside. Several examples have demonstrated biological activity,^{3,5} including in vivo activity against the murine L-1210 tumor, and cytostatic activity against *Streptococcus faecalis* and the K-12 strain of *Escherichia coli*. The clinically useful antiviral drug 9-(2-hydroxyethoxymethyl)guanine (Acyclovir, Zovirax)^{6,7} is a guanine derivative bearing a truncated, acyclic chain in place of the β-D-ribofuranosyl group in the natural nucleoside guanosine. The objective of the present work was to prepare a series of thymine derivatives having attached at

N-1 the four D-pentoses in acyclic form, initially linking an acyclic 1-bromo-1-ethylthio acetylated derivative of the sugar to the heterocycle to generate a diastereomeric pair of 1-ethylthio-1-(thymine-1-yl) derivatives, which were individually characterized, and then removing the ethylthio group by a free-radical procedure, ultimately to yield the title compounds.

2. Results and discussion

2.1. Synthesis

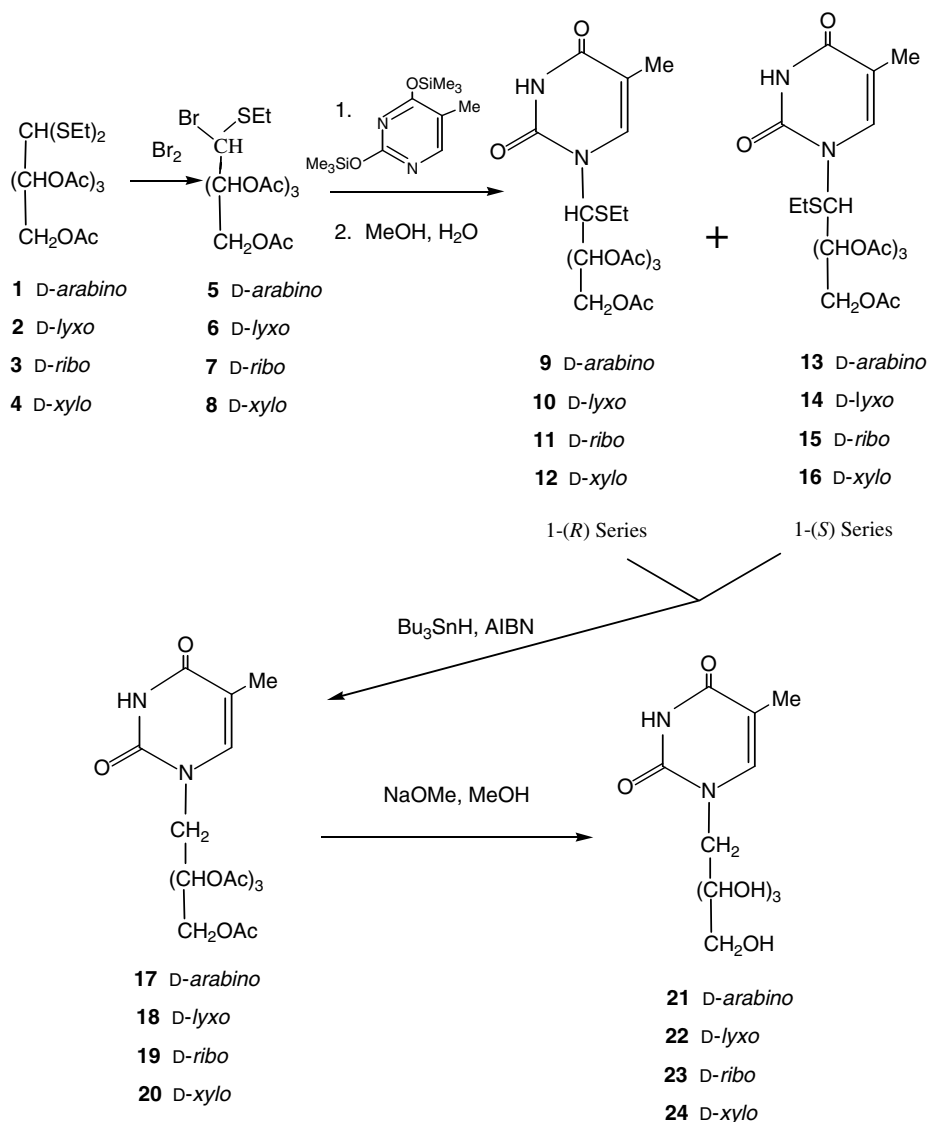
The starting compounds were the peracetylated diethyl dithioacetals (**1–4**) of D-arabinose, D-lyxose, D-ribose, and D-xylose, respectively. Treatment of these compounds with one molar equivalent of bromine in cold diethyl ether, following the precedent of Gauthier,⁸ Weygand and associates,⁹ and our earlier work^{1–4} converted each dithioacetal into a product of lower TLC mobility through replacement of one ethylthio group by bromine and affording, after removal of volatile materials, the corresponding 1-bromo-1-ethylthio derivatives **5–8**, respectively, as syrups that were unstable on storage

* Corresponding author. Tel.: +1 202 885 1767; fax: +1 202 885 1095; e-mail: carbchm@american.edu

and were used directly in the next step. The fusion coupling procedure of Nishimura and co-workers^{10,11} was employed. Each of the bromo derivatives was mixed with 1 equiv of 2,4-bis(trimethylsilyl)thymine¹² and heated in a sealed tube to 140 °C, and the fused mixture was maintained at this temperature for 45 min, resulting in nucleophilic attack by N-1 on C-1 of the sugar derivative and elimination of bromotrimethylsilane. The coupled products, still having a trimethylsilyloxy group at C-4 of the pyrimidine, were subjected to an aqueous methanolic isolation procedure to remove the remaining trimethylsilyl group and afford a C-1' diastereomeric pair of nucleoside derivatives in each of the four series.

as a levorotatory oil identified as the (1'*S*) isomer **13**. In similar fashion, the *D*-lyxo bromide **6** afforded in 48% yield a 1:1.2 diastereomeric mixture that was resolved chromatographically to afford 19% of the faster-migrating isomer as a levorotatory foam identified as the (1'*S*) diastereomer **14** and 23% of a dextrorotatory oil identified as the (1'*R*) diastereomer **10**.

Likewise, the *D*-ribo bromide **7** gave 82% of a 1:3.1 diastereomeric mixture that afforded 8% of the crystalline, minor, dextrorotatory (1'*R*) isomer **11** and 23% of the syrupy, levorotatory major isomer, the (1'*S*) product **15**. Finally, the *D*-xylo bromide **8** (which was particularly unstable and was used without delay) gave 49%



From the *D*-arabino bromide **5**, there was obtained in 41% yield a 3.7:1 mixture of diastereomers that were separated by column chromatography on silica gel to yield 21% of the faster-migrating, crystalline major diastereomer as a strongly dextrorotatory product identified as the (1'*R*) isomer **9**, and the minor isomer (5%)

of a 2.2:1 mixture of diastereomers, which on chromatographic resolution yielded a faster-migrating, levorotatory component, obtained crystalline in 22% yield and identified as the (1'*S*) isomer **16**, along with 7% of a dextrorotatory product identified as the (1'*R*) isomer **12**.

All of the products **9–16** were chromatographically homogeneous and gave satisfactory elemental analyses, most commonly as the hemihydrated form. Their electron-impact mass spectra were all essentially identical, showing small molecular-ion (m/z 488.4) and $M+1$ peaks, along with significant peaks arising through C-1'-N-1 cleavage at m/z 127 for the protonated base and m/z 363 for the acyclic sugar cation. Loss of the ethylthio group generates a major ion at m/z 427, which by loss of ketene gives a cation at m/z 385. Other fragments attributable to the sugar chain were also observed in the mass spectra of the starting dithioacetals **1–4**. Complete details of the mass spectra are recorded elsewhere.¹³

Tables 1 and 3 record ¹H and ¹³C NMR data, respectively, and proton-proton spin-coupling data are recorded in Table 4. The H-1' resonances predictably fall at lower field (~6 ppm) than the remaining proton signals of the chain, and likewise the C-1' resonances near 60 ppm lie at lower field than the remaining carbon signals. Most importantly, the NMR data provide confirmation that the coupling reaction leads to attachment of the sugar chain to N-1 and not to N-3 of the pyrimidine. Had the attachment been at N-3, the resonance of the proton at N-1 would have shown splitting through coupling to the vicinal H-6, and concurrently the H-6 resonance would be split by the proton at N-1 and the distal allylic methyl group at C-5. In fact, however, the NH proton signal is observed as a singlet, broadened by the quadrupolar effect of N-3, and not as a broadened doublet. The lack of splitting of this signal is a clear evidence of attachment of the sugar chain to N-1 of the heterocycle. Furthermore, the H-6 resonance is observed as a narrow (~1 Hz) doublet (and not as an ABX splitting pattern) coupled to the methyl group at C-5.

Additional evidence for the chain attachment at N-1 is provided by UV spectral data. Thymine derivatives alkylated at N-1 show maximal absorption¹⁴ at lower wavelength than those alkylated at N-3; thus 1,5-dimethyluracil near neutral pH shows λ_{max} at 272 nm, whereas 3,5-dimethyluracil shows maximal absorbance at 264.5 nm. The nucleoside derivatives **9–16** exhibit maximal absorbance in the 272–276 nm range, further supportive of the N-1 substitution assignment.

Earlier efforts to remove the ethylthio group from acyclic-sugar nucleosides similar to compounds **9–16** by a variety of reagents have in all instances led to cleavage of the sugar-base linkage,¹⁵ but a free-radical procedure has subsequently been shown to be successful in application with acyclic-sugar purine nucleosides.¹⁶ In the present work it was found that the individual epimers **9** or **13**, on treatment with 4–6 equiv of tributylstannane in the presence of azobisisobutanonitrile (AIBN) in boiling toluene for 8–12 h, led to clean removal of the ethylthio group to afford the acetylated 1-*N*-(1-deoxy-*D*-arabinitol-1-yl)thymine **17**. The same procedure conducted with the mixed pairs of epimers in the *arabino* (**9** + **13**), *lyxo* (**10** + **14**), *ribo* (**11** + **15**), and *xylo* (**12** + **16**) series afforded the corresponding acetylated alditol-1-yl nucleosides **17–20** in 93, 82, 93, and 92% yields, respectively. The electron-impact mass spectra of these products all showed small molecular-ion peaks at m/z 428 and fragments m/z 126 and 127 from C-1'-N-1 cleavage, along with additional fragments listed elsewhere.¹³ The ¹H NMR spectra of **17–20** (Table 1) showed for the methylene protons at C-1' the anticipated upfield shift (~2 ppm) and changed multiplicity with respect to H-1 of the 1'-ethylthio precursors **9–16**, along with a comparable upfield shift (~10 ppm) of the corresponding ¹³C resonances for C-1' (Table 3).

Conventional Zemplén catalytic deacetylation of the tetraacetates **17–20** by methanolic sodium methoxide afforded in high yield the corresponding free tetrols **21–24** as high-melting crystalline solids. The *arabino* (**21**), *lyxo* (**22**), and *xylo* (**24**) derivatives were hemihydrates and the *ribo* derivative (**23**) was a nonhydrated, as indicated by microanalytical data. The ¹³C resonances for C-1' (attachment to nitrogen) in **21–24** were predictably less deshielded than those of C-5' (attachment to oxygen) (Table 3).

The chirality at C-1' in compounds **9–16** was assigned on the basis of the Generalized Heterocycle Rule,¹⁷ which attributes a dominant rotatory contribution to the atom (C-1' in this instance) having attached to it both a heterocycle and a chalcogen. By this rationale, the C-1' epimers having strongly positive specific rotations at the sodium D line (**9–12**) are the (1'*R*) isomers, and those exhibiting corresponding levorotation (**13–16**)

Table 1. ¹H NMR Chemical shifts (400 MHz, CHCl₃; ppm relative to Me₄Si) for compounds **9–16**

Compound	H-1'	H-2'	H-3'	H-4'	H-5a'	H-5b'	H-6	CH ₃	N-H	SCH ₂	CH ₂ CH ₃	OAc
9	5.96d	5.42dd	5.25dd	5.12m	4.24dd	4.03dd	7.36d	1.99d	8.93br s	2.52q	1.25t	2.03, 2.08, 2.13, 2.14
10	6.05d	5.55dd	5.03dd	5.27m	4.23dd	3.71dd	7.37d	1.93d	8.97br s	2.48q	1.19t	1.94, 2.02, 2.07, 2.08
11	6.17d	5.56dd	5.32dd	5.31m	4.10dd	4.26dd	7.35d	1.89d	9.10br s	2.51q	1.23t	1.97, 1.99, 2.04, 2.10
12	5.98d	5.25dd	5.50dd	5.29m	4.06dd	4.27dd	7.37 ^a	1.94 ^a	9.04br s	2.54q	1.24t	2.05, 2.06, 2.08, 2.13
13	5.88d	5.63dd	5.27dd	5.07m	4.05dd	4.25dd	7.33d	1.92d	9.21br s	2.52q	1.23t	1.97, 2.04, 2.05, 2.19
14	6.05d	5.55dd	5.02dd	5.27m	4.23dd	3.71dd	7.37d	1.93d	8.97br s	2.48q	1.19t	1.94, 2.02, 2.07, 2.08
15	5.98d	5.25dd	5.50dd	5.29m	4.06dd	4.27dd	7.37a	1.94	9.04br s	2.54q	1.24t	2.05, 2.06, 2.08, 2.13
16	5.72d	5.48dd	5.36dd	5.44m	4.28dd	3.98dd	7.53a	1.92a	8.98br s	2.53q	1.24t	2.02, 2.03, 2.05, 2.17

^a Denotes an incompletely resolved signal.

are the (1'*S*) isomers. Although this criterion is not totally unambiguous, the closely related 1-fluoro analogue of compound **9** (whose stereochemistry at C-1' has been definitively assigned on the basis of an X-ray crystallographic study)³ has a specific rotation of +132° at the sodium D line. This value is practically identical to that (+135°) for compound **9**, lending strong support to the assignments made here for **9**, and by extension, for the complete series **9–16**. Comparable correlations between crystallographic and polarimetric data have been made in related examples.¹⁸

spectroscopy was used to determine vicinal and geminal proton–proton coupling constants for all nucleoside analogues prepared in this study and the data are recorded in Table 4, chloroform-*d* being used as a solvent for all except tetrols **21–24**, for which D₂O was the solvent. Conformational attributions were made, following earlier precedent^{19–21} on the concept of a time-averaged dynamic equilibrium between all possible rotameric states, with a large (~9 Hz) vicinal coupling indicating principally anti disposition of vicinal protons, a small (~2 Hz) coupling being indicative of gauche disposition,

Table 2. ¹H NMR Chemical shifts (400 MHz, CHCl₃; ppm relative to Me₄Si) for compounds **17–20** and (400 MHz, D₂O; ppm relative to DSS) for compounds **21–24**

Compound	H-1'a	H-1'b	H-2'	H-3'	H-4'	H-5a'	H-5b'	H-6	CH ₃	N-H	OAc
17	3.32dd	4.13d	5.08m	5.36dd	5.50m	4.09dd	4.18dd	6.89d	1.83d	8.96br s	1.95, 1.99, 2.01, 2.12
18	3.51dd	4.13dd	5.24m	5.27dd	5.36m	3.94dd	4.23dd	6.88 ^a	1.87 ^a	9.03br s	1.98, 2.02, 2.06, 2.15
19	3.61d	4.15dd	5.20m	5.26dd	5.27m	4.09dd	4.26dd	6.94d	1.82d	10.00br s	1.96, 1.99, 2.06, 2.09
20	2.89d	3.51dd	5.30m	4.12dd	5.41m	3.97dd	4.31dd	6.91 ^a	1.85 ^a	9.61br s	2.01, 2.02, 2.09, 2.10
21	3.81dd	3.98dd	3.75m	3.52dd	4.18m	3.65dd	3.85dd	7.48s	1.87s		
22	3.52dd ^a	4.21dd ^a	3.55m ^a	3.39dd ^a	3.78m ^a	3.52dd ^a	3.82dd ^a	7.35s	1.74s		
23	3.64dd	4.02dd	3.67m	3.57dd	3.90m	3.51dd	3.58dd	7.31s	1.73s		
24	3.59m ^a	3.88m ^a	3.59m ^a	3.59m ^a	3.88m ^a	3.59m ^a	3.59m ^a	7.32s	1.73s		

^a Denotes an incompletely resolved signal.

Table 3. ¹³C NMR Chemical shifts (75 MHz, CHCl₃; ppm relative to Me₄Si) for compounds **9–20** and (75 MHz, D₂O; ppm relative to DSS) for compounds **21–24**

Compound	C-1'	C-2'	C-3'	C-4'	C-5'	C-2	C-4	C-5	C-6	6-CH ₃	CH ₂	CH ₃	C=O	OCH ₃
9	59.51	70.02	67.65	68.32	61.77	151.07	163.15	112.88	135.41	12.58	25.21	14.16	170.01, 170.14, 170.74	20.54, 20.78
10	55.31	71.43	69.41	69.32	69.63	151.40	165.43	113.18	137.97	14.46	27.27	16.06	171.05, 171.91, 172.19	22.39, 22.52, 22.57, 22.61
11	58.30	72.31	69.61	69.50	62.15	151.61	163.85	112.22	137.05	13.11	25.63	14.86	169.54, 169.89, 170.32, 171.03	20.91, 21.10, 21.32
12	61.82	70.44	68.86	69.59	61.82	151.31	163.80	111.55	137.05	12.40	25.58	14.22	169.59, 169.89, 170.20, 170.62	20.35, 20.60
13	58.18	69.53	68.32	68.56	61.70	151.38	163.70	111.49	136.93	12.34	25.39	14.28	169.95, 170.74	20.17, 20.54, 20.66
14	62.63	70.82	68.77	68.02	62.72	151.40	165.43	113.18	138.56	13.43	25.41	14.71	169.58, 170.43, 172.32	20.93, 21.07, 21.20
15	60.51	74.87	68.63	68.42	59.29	146.33	164.48	126.04	137.08	11.61	25.94	13.22	171.77, 171.79	19.56, 19.65, 19.81
16	60.00	71.84	68.14	69.84	61.57	150.77	163.51	111.30	135.89	12.46	25.51	14.10	169.65, 169.95, 170.62, 170.86	20.29, 20.41, 20.66
17	50.13	n.o.	68.89	69.56	62.46	151.83	165.06	111.82	141.02	12.98			171.08	21.48
18	48.79	70.14	68.54	68.89	62.03	151.63	164.41	111.25	140.68	12.68			169.93, 170.48, 170.56, 170.88	21.01, 21.06, 21.10, 21.14
19	47.99	69.93	69.35	68.84	62.04	151.34	164.91	110.91	140.88	12.55			170.03, 170.22, 170.46, 170.95	20.98, 21.04, 21.19, 21.36
20	48.88	76.69	69.09	69.64	61.87	151.06	164.36	111.05	140.37	12.21			170.06, 170.18, 170.49, 170.79	20.64, 20.77
21	41.43	54.50	57.09	65.68	62.46	155.23	169.87	113.06	146.67	17.70				
22	n.o.	50.00	61.22	70.05	68.45	150.91	165.46	108.59	142.55	9.66				
23	38.51	50.61	62.25	72.66	69.21	143.93	165.31	110.07	138.05	11.12				
24	n.o.	51.78	62.69	69.64	69.33	152.70q	167.33	110.57	140.37	11.57				

n.o. Not observed.

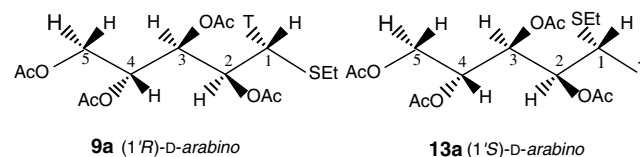
2.2. Conformational studies

High-field NMR spectroscopy in conjunction with selective proton decoupling and two-dimensional correlation

and intermediate coupling values being consistent with substantial population of more than one rotameric state. The extended planar zigzag (*P*) conformation favored for a linear alkane chain on the basis of maximal

separation of large groups along each carbon–carbon bond is subject to perturbation in polysubstituted systems,^{19–21} notably by unfavorable parallel 1,3-interactions between bulky substituents as well as by polar effects and by solvent interactions. Polysubstituted systems may thus favor nonextended (sickle, gauche, *G*) conformations or conformational mixtures, according to the substitution mode. Particular *G* conformations derived by 120° rotation of the *P* form about a particular bond are designated²¹ by the lower-numbered atom and the sign of rotation when viewed from the remote atom; thus ${}_3G^+$ denotes the conformation derived from the *P* conformation by 120° clockwise rotation of the remote atom along the C-3–C-4 bond.

thy that in each epimer the rotameric preference along the C-1'–C-2' bond is the one that avoids bringing a bulky group (heterocycle or SEt) in 1,3-parallel disposition with the acetoxy group at C-3'.



This behavior of these two epimers having the *arabino* configuration, showing a strong preference for the *P*

Table 4. Proton–proton NMR spin-coupling data (400 MHz, CDCl₃; Hz) for compounds **9–20** and (400 MHz, D₂O; Hz) for compounds **21–24**

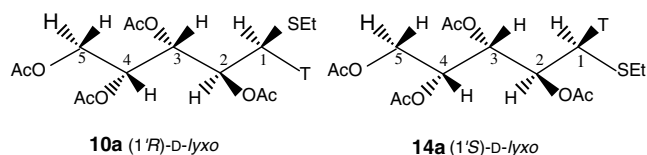
Compound	$J_{1',2'}$	$J_{1a',2'}$	$J_{1b',2'}$	$J_{2',3'}$	$J_{3',4'}$	$J_{4',5a'}$	$J_{4',5b'}$	$J_{5a',5b'}$	$J_{1a',1b'}$	$J_{Me,6}$
9	8.4			3.0	8.4	2.7	5.7	12.3		1.2
10	2.5			9.8	2.0	5.3	7.6	11.6		0.9
11	9.1			2.5	9.3	5.4	2.4	12.2		1.3
12	7.8			3.9	5.9	5.4	3.9	11.7		^a
13	8.8			2.9	8.8	2.9	5.9	12.7		1.0
14	4.0			9.3	2.2	4.5	7.6	11.8		1.0
15	8.3			2.8	9.1	7.1	3.3	11.9		^a
16	4.9			6.8	3.9	4.4	6.8	11.7		^a
17		9.8	2.7	2.3	9.1	4.3	2.5	12.7	14.4	
18		8.6	2.8	7.1	3.3	6.8	5.3	11.6	14.6	
19		8.9	2.1	3.9	8.8	5.7	3.0	12.3	14.5	
20		3.0	8.8	4.2	2.9	5.7	3.7	12.0	14.4	
21		9.1	4.0	1.1	8.8	6.2	9.1	11.7	14.1	
22		^a	^a							
23		7.1	2.6	8.8	2.8	7.1	5.9	12.1	14.3	
24		^a	^a	^a						

^a Incompletely resolved signal.

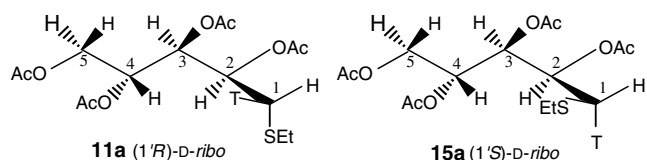
2.2.1. 2,3,4,5-Tetra-*O*-acetyl-1-deoxy-1-*S*-ethyl-1-thio-1-(thymine-1-yl)-aldehydo-*D*-pentose aldehydols—(1'*R*)- and (1'*S*)-*D*-arabino epimers (9** and **13**).** The spectra of both epimers were amenable to first-order analysis and proton assignments paralleled those made earlier^{3,5} for peracetylated 1-*S*-alkyl-1-(pyrimidin-1-yl)-1-thiopentitols. The H-1 resonance for the dextrorotatory epimer **9** was a wide doublet ($J_{1',2'}$ 8.4 Hz) at δ 5.96, and that for the levorotatory epimer **13** observed at δ 5.88 was likewise a wide doublet ($J_{1',2'}$ 8.8 Hz), indicating that H-1' and H-2' are essentially antiparallel in both epimers. The $J_{2',3'}$ values for **9** and **13** are 3.0 and 2.9 Hz, respectively, indicating an essentially gauche disposition between H-2' and H-3', while the respective $J_{3',4'}$ values are 8.4 and 8.8 Hz, consistent with the essentially antiparallel disposition of H-3' and H-4'. These data indicate that each epimer strongly favors a fully extended, planar zigzag conformation having all backbone carbon atoms in the same plane. The (1'*R*) epimer has the SEt group also in that plane, as indicated in structure **9a**, whereas in the (1'*S*) epimer the heterocycle occupies the extended orientation, as shown in **13a**. It is noteworthy

that in each epimer the rotameric preference along the C-1'–C-2' bond is the one that avoids bringing a bulky group (heterocycle or SEt) in 1,3-parallel orientation with the acetoxy group at C-3'.

2.2.2. (1'*R*)- and (1'*S*)-*D*-lyxo epimers (10** and **14**).** Analysis of the spectra of both epimers was essentially first order, but minor differences in the $J_{1',2'}$ couplings were evident. The H-1' signal for the (1'*R*) epimer **10** was a narrow doublet ($J_{1',2'}$ 2.5 Hz) consistent with the gauche disposition of H-1' and H-2', whereas that for the (1'*S*) epimer **14** showed a $J_{1',2'}$ value of 4.0 Hz, indicating a major but not exclusive contribution of the H-1'–H-2' gauche rotamer. For both epimers, the $J_{2',3'}$ and $J_{3',4'}$ values were similar (9.8 and 2.0 Hz, respectively, for **10** and 9.3 and 2.2 Hz, respectively, for **14**), indicating the extended planar (*P*) orientation of the carbon backbone for each epimer. The rotameric state along the C-1'–C-2' bond in each epimer is consistent with avoidance of that rotamer that would place a large C-1' substituent (heterocycle or SEt) in 1,3-parallel orientation with the acetoxy group at C-3', leading to the favored conformations depicted in **10a** and **14a**.

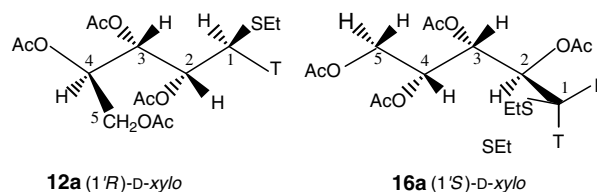


2.2.3. (1'*R*)- and (1'*S*)-D-ribo epimers (11 and 15). For the (1'*R*) epimer 11 the H-1' signal is a wide doublet with $J_{1',2'}$ 9.1 Hz, indicating antiperiplanar disposition of H-1' and H-2', and the disposition of H-3' and H-4' is likewise antiperiplanar ($J_{3',4'}$ 9.3 Hz), whereas H-2' and H-3' are gauche-disposed ($J_{2',3'}$ 2.5 Hz). Very similar parameters are observed for the (1'*S*) epimer 15, with $J_{1',2'}$ 8.3 Hz, $J_{2',3'}$ 2.8 Hz, and $J_{3',4'}$ 9.1 Hz, indicating essentially similar favored conformations for both epimers, with rotation from about the C-2'–C-3' bond to alleviate the 1,3-parallel interaction between the acetoxy groups at C-2' and C-4' that would have been present in the *P* conformation. This brings C-1' out of the plane of the rest of the backbone chain. Again, as in the two preceding examples, the favored rotameric state about the C-1'–C-2' bond is the one that does not generate a 1,3-parallel interaction between the 3'-OAc group and either the heterocycle or the SET group, and the favored conformations are thus the ${}_2G^-$ conformers depicted as **11a** and **15a**.



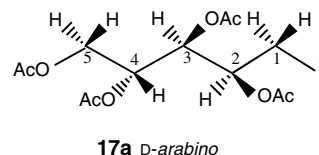
2.2.4. (1'*R*)- and (1'*S*)-D-xylo epimers (12 and 16). The vicinal proton–proton couplings for both epimers deviate significantly from those values diagnostic of preponderantly antiperiplanar or gauche, and are indicative of conformational mixtures²² with substantial contributions from more than one conformer. The $J_{1',2'}$ value of 7.8 Hz for the (1'*R*) epimer **12** is consistent with a major contribution from the antiperiplanar orientation of H-1' and H-2', but the $J_{1',2'}$ coupling of 4.9 Hz for the (1'*S*) epimer **16** indicates comparably weighted contributions from antiperiplanar and gauche dispositions of these protons. Likewise the respective $J_{2',3'}$ and $J_{3',4'}$ values are 3.9 and 5.9 Hz for the (1'*R*) epimer **12**, and 6.8 and 3.9 Hz for the (1'*S*) epimer **16**, again demonstrating conformational mixing with no clear single, principal conformation for either epimer. Avoidance of the 1,3-parallel interaction of the acetoxy groups at C-2' and C-4' that would have been present in the *P* conformation again would seem to be the driving force in establishing the most favored disposition of these epimers, and from the possible contributors to the equilibrium population, a major contributor for the (1'*R*) epimer appears to be the ${}_3G^+$ conformer

shown as **12a**, and that for the (1'*S*) epimer the ${}_2G^-$ conformer shown as **16a**. Again, the rotameric populations about the C-1'–C-2' bond favor the orientation that minimizes steric interactions of the heterocycle and SET groups.



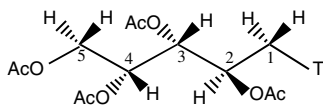
2.2.5. 2,3,4,5-Tetra-*O*-acetyl-1-deoxy-1-(thymine-1-yl)-D-pentitols (17–20). Removal of the ethylthio group from the precursors **9–16** led to loss of the downfield H-1' resonance near 6 ppm (Table 1) and the appearance some 2 ppm further upfield of a two-proton AB portion of an ABX system for the methylene group at C-1' (Table 2). A second AB portion of an ABX system, somewhat downfield of the C-1' methylene resonances, is attributable to the C-5' methylene protons, whose chemical shifts are little changed from their positions in the ethylthio precursors. The C-5' methylene protons remain subject to the same level of deshielding by the adjacent oxygen substituent, whereas the less electronegative nitrogen atom of the thymine substituent causes the C-1' methylene protons to resonate at somewhat higher field. Based on these assignments, the proton–proton coupling constants could be extracted (Table 4), and the conformational behavior for compounds **17–20** determined.

2.2.6. D-arabino Isomer (17). The observed values for $J_{2',3'}$ (2.3 Hz) and $J_{3',4'}$ (9.1 Hz) give clear support for the extended planar zigzag (*P*) conformation for **17**, and the respective small (2.7 Hz) and large (9.8 Hz) couplings of the C-1' methylene protons with H-2' are consistent with the thymine N-1 atom lying in the same plane as the carbon atoms of the chain, and the fully extended conformation **17a** depicted is clearly the favored form.



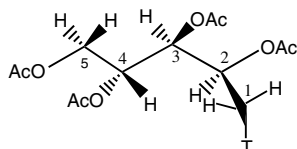
2.2.7. D-lyxo Isomer (18). The conformationally diagnostic spin couplings for compound **18** show, respectively, large (7.1 Hz) and small (3.3 Hz) values for $J_{2',3'}$ and $J_{3',4'}$ and the magnetically nonequivalent protons at C-1' show large (8.6 Hz) and small (2.8 Hz) couplings with H-2', leading to assignment of the *P* conformation depicted in **18a**, as the most favored, but not exclusive, form; the observed $J_{2',3'}$ and $J_{3',4'}$ values are not at the

limits expected for exclusive antiperiplanar and gauche dispositions, respectively.



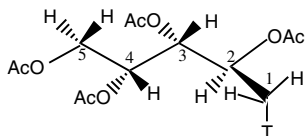
18a *D*-lyxo

2.2.8. *D*-ribo Isomer (19). The large (8.8 Hz) value of $J_{3',4'}$ is consistent with essentially exclusive antiperiplanar orientation of H-3' and H-4', but the $J_{2',3'}$ value of 3.9 Hz is indicative of conformational instability²² with an appreciable contribution of both the *P* conformer having H-2' and H-3' antiperiplanar, and a larger contribution of the ${}_2G^-$ gauche form illustrated (**19a**), arising through rotation about the C-2'–C-3' bond to alleviate the 1,3-interaction between acetoxy groups at C-2' and C-4'. As with the preceding two examples, the large (8.9 Hz) and small (2.1 Hz) between the methylene protons at C-1' and H-2' establish that H-2 is antiperiplanar to one of the C-1 hydrogen atoms.



19a *D*-ribo

2.2.9. *D*-xylo Isomer (20). The key diagnostic couplings, $J_{2',3'}$ and $J_{3',4'}$, are, respectively, 4.2 and 2.9 Hz, and the latter indicates that H-3' and H-4' are preponderantly gauche, but the former is indicative of conformational instability with rotation about the C-2'–C-3' bond to alleviate the 1,3-parallel interaction between the acetoxy groups at C-2' and C-4' in the *P* conformation, and generating the ${}_2G^-$ conformer illustrated as **20a** as a significant contributor to the conformational equilibrium.

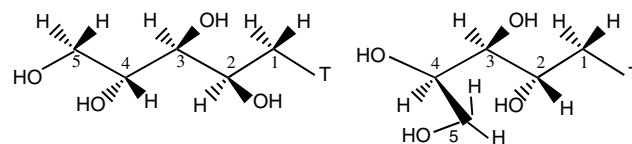


20a *D*-xylo

2.2.10. 1-Deoxy-1-(thymine-1-yl)-*D*-pentitols (21–24). Removal of the ester substituents from **16** to **20** caused significant compression of the signals of the backbone protons into a narrow range, and selective decoupling together with COSY experiments was required to assign individual resonances and determine vicinal coupling constants. This proved possible for *D*-arabino and *D*-ribo tetrols **21** and **23**, but extensive signal overlap in the spectra of *D*-lyxo and *D*-xylo tetrols **22** and **24** precluded specific assignments, even with the addition of small

amounts of praseodymium chloride, an effective shift reagent,²¹ to the D₂O solution.

For the *D*-arabino tetrol **21**, the small $J_{2',3'}$ coupling supports the gauche disposition of H-2' and H-3', while the value (8.8 Hz) of $J_{3',4'}$ indicates antiperiplanar relationship between H-3' and H-4', and the *P* conformation depicted (**21a**) can be assigned as the major conformer. For *D*-ribo tetrol **23**, the $J_{2',3'}$ and $J_{3',4'}$ couplings are, respectively, 8.8 and 2.8 Hz, and indicate the ${}_3G^+$ conformer depicted (**23a**) as the major contributor to the conformational equilibrium, and a mixture of rotamers along C-4'–C-5' that favors O-5' oriented antiperiplanar to C-3'.



21a *D*-arabino

23a *D*-ribo

2.3. Molecular modeling studies

An attempt was made to match the conformational properties determined here from NMR data for the tetraacetates **16–20** and the free tetrols **21–14** with minimum-energy conformations predicted by molecular modeling. The calculations were performed using Hyperchem[®] Release 5 for Windows, and were initiated from the planar zigzag (*P*) conformation. In the simulations for the tetrols the AMBER force field was employed using the Polak–Ribiere minimization algorithm, and simulations for the tetraacetates required use of the MM⁺ force field. Full details are presented in Ref. 13.

The results overall showed no consistent agreement with the conformations demonstrated by NMR experimental studies, not even in the most qualitative sense. It appears that the software used was not capable of finding the global energy minima through sequential rotation of intramolecular bonds, and presumably traps the computed energy into false local minima. It may be possible with use of more robust modeling software to find reliably the true global energy minima, but the results here emphasize the need for caution in using popular software as a tool for predicting conformational properties in the absence of direct experimental data.

2.4. Biological studies

The four acyclic-sugar nucleosides **21–24** were tested for activity against typical plant viruses and a fungus. At application levels of 100 ppm, all four compounds were toxic to cucumber and tobacco plants, while rice plants tolerated the compounds at levels of 100 ppm. The four compounds were evaluated at levels of 10, 25, and

50 ppm for their ability to combat infection by the tobacco mosaic virus in tobacco plants, and by the Cucumber Green Mottle Mosaic Virus in cucumber plants, and they showed no activity.

Tested against the rice blast fungus *Pyricularia oryzae*, the four compounds demonstrated biological activity that varied according to their stereochemical configuration, with the *D-ribo* derivative **23** showing the greatest activity. At the 10 ppm application level, the *D-arabino* and *D-lyxo* derivatives **21** and **22** showed no activity, while the *D-xylo* derivative **24** actually enhanced the development of the fungal symptoms (PV = 127), whereas the *D-ribo* derivative **23** showed significant inhibition of the pathogen (PV = 71). At the 50 ppm application level, compounds **21** and **23** showed some inhibitory activity, but at the 100 ppm level the *D-ribo* compound **23** actually enhanced the fungal activity. Details are recorded in Table 5.

Table 5. Protective values^a (PV, %) of compounds **21**, **22**, **23**, and **24** and a control at three concentrations versus development of *Pyricularia oryzae* symptoms in potted rice plants

Compound	Concentration (ppm)		
	10	50	100
21	103	82	162
22	105	123	118
23	71	84	203
24	127	101	105
Control	100	100	100

^a PV = average number of lesions in treated leaves × 100/average number of lesions in nontreated leaves. Full details are recorded in Ref. 13.

3. Experimental

3.1. General methods

Infrared spectra were recorded with a Shimadzu FTIR-8300 Fourier-transform infrared spectrophotometer, and UV spectra with a Hewlett–Packard Diode Array Spectrophotometer Model 8452A. Optical rotations (sodium D line) were measured with a Perkin–Elmer Model 141 polarimeter. Electron-impact mass spectra were obtained with a Shimadzu GCMS QP5050A gas chromatograph–mass spectrometer at an ionization potential of 70 eV and an accelerating potential of 1.50 kV. The column employed for all GLC analyses was a 30 m × 0.25 mm Supelco fused-silica capillary (PTE™-5, 0.25 μm film). The carrier gas was set to flow at 50.00 mL/min with a split ratio of 30.00. The sample was applied through the injector (180 °C) and to the column at an initial temperature of 60.0 °C. The column temperature was then elevated at 10 °C/min until the final oven temperature of 280.0 °C was reached. Nuclear magnetic resonance (NMR) spectra were obtained using a Bruker Avance DRX₄₀₀ NMR instrument at 400 MHz

for ¹H spectra and 75 MHz for ¹³C spectra. Chemical shifts are referenced to that of Me₄Si (0.0 ppm) for solutions in CDCl₃ (**9–20**) and with sodium 4,4-dimethyl-4-silapentanesulfonate (DSS) for solutions in D₂O (**21–24**). Assignments of signals were made by first-order analysis of spectra and the assignments were supported by two-dimensional correlation spectroscopy (COSY) and homonuclear decoupling experiments (40–60 dB), using commercial software supplied with the spectrometer (XWIN NMR Acquisition and XWIN NMR Processing). Elemental analyses were performed by Atlantic Microlab, Inc. All reactions were monitored by silica gel (Whatman Al SIL G/UV, 250 μm thickness) thin-layer chromatography (TLC) and detection was accomplished by either UV absorption and/or charring effected with 5% H₂SO₄ in EtOH. Preparative chromatography was performed using Whatman PKGF silica gel 60A (1000 μm thickness). In all cases, column chromatography was performed using Kieselgel 60 (70–230 mesh ASTM).

3.2. Preparation of 2,4-bis(trimethylsilyl)thymine¹²

To a magnetically stirred suspension of thymine (12.6 g, 0.100 mol) in 300 mL of dry toluene was added 23.0 g (2.1 equiv) of chlorotrimethylsilane. The flask was fitted with an addition funnel, which was used to add 30.0 mL of Et₃N (2.5 equiv) in 30 mL of toluene and the mixture was stirred overnight. The mixture was filtered and the filtrate washed with three 25-mL portions of toluene. The solvent was then removed by simple distillation and the product isolated by vacuum distillation (124 °C/13 mmHg). The purified product crystallized upon being kept for several hours and was sufficiently pure for subsequent condensation reactions; yield 21.2 g (78.4%).

3.3. Preparation of 2,3,4,5-tetra-*O*-acetyl-1-bromo-1-deoxy-1-*S*-ethyl-1-thio-aldehydo-*D*-arabinose aldehydrol (**5**)²

2,3,4,5-Tetra-*O*-acetyl-*D*-arabinose diethyl dithioacetal²³ (**1**, 2.15 g, 5.06 mmol) was dissolved in 25 mL of anhydrous diethyl ether in a sealed flask fitted with a thermometer, a septum, and a magnetic stirring device. To the solution was added 0.27 mL (1.05 equiv) of Br₂, at such a rate that the temperature remained below 10 °C. The reaction was monitored by TLC (3:1 toluene–MeOH) for 40 min at which time TLC showed the absence of starting material and the appearance of a single, more-slowly moving spot detectable by H₂SO₄ charring. The volatile materials were evaporated off using a vacuum source and the residue was washed twice with diethyl ether to yield **5** as a pale-yellow syrup; *R*_f 0.44 (3:1 toluene–MeOH). The product was not stable on storage and was used without delay in the next step.

3.4. (1*R,S*)-2,3,4,5-Tetra-*O*-acetyl-1-deoxy-1-*S*-ethyl-1-thio-1-(thymine-1-yl)-aldehydo-*D*-arabinose aldehydols (**9** and **13**)

To 4.72 g (10.1 mmol) of freshly prepared 2,3,4,5-tetra-*O*-acetyl-1-bromo-1-deoxy-1-*S*-ethyl-1-thio-1-aldehydo-*D*-arabinose aldehydrol (**5**) in a pressure reaction tube (Ace Glass, Inc.) was added 2.74 g (1.0 equiv) of 2,4-bis(trimethylsilyl)thymine in 25 mL of dry toluene. The tube was sealed and the mixture heated in an oil bath for 8 h at 140 °C. The darkened residue was then removed and allowed to cool to room temperature. The pressure was then carefully released and the mixture triturated with 15 mL of 4:1 MeOH–water and then CHCl₃ (50 mL). The mixture was filtered and the filtrate washed with distilled water, and dried (MgSO₄). The solution was decolorized with activated charcoal to yield a pale-yellow solution. TLC (2:1 EtOAc–hexane) showed two major products that were detectable by both UV absorbance and H₂SO₄ charring. Evaporation of the solvent yielded 4.40 g of yellow syrup; crude yield 89%. Analysis by GLC–MS indicated two products with identical mass spectra and retention times of 24.1 and 24.6 min, interpreted as the diastereomeric products **9** and **13** in the ratio of 3.7:1.0. Column chromatographic purification on silica gel afforded 3.20 g of the mixed diastereomers **11a** and **11b**, as a white foam; yield 65%.

3.4.1. (1*R*)-2,3,4,5-Tetra-*O*-acetyl-1-deoxy-1-*S*-ethyl-1-thio-1-(thymine-1-yl)-aldehydo-*D*-arabinose aldehydrol (**9**).

The aforementioned foam (3.20 g) was dissolved in a minimal amount of EtOAc and applied to a column (3.0 cm×60 cm) of silica gel (200 g). The column was eluted with 2:1 EtOAc–hexane, and concentration of the fractions having *R*_f 0.48 afforded **9** as a white foam that crystallized from pure EtOH; yield 2.07 g (42%); mp 126.0 °C, [α]_D²⁵ +135 (CHCl₃); *R*_f 0.48 (2:1 EtOAc–hexane); EIMS: *m/z* 488 [M]. Anal. Calcd for C₂₀H₂₈N₂O₁₀S·0.5H₂O: C, 48.27; H, 5.89; N, 5.63; S, 6.44. Found: C, 48.48; H, 5.71; N, 5.81; S, 6.48. ¹H NMR and ¹³C NMR chemical shifts, and proton–proton coupling constants are given in Tables 1, 3, and 4, respectively.

3.4.2. (1*S*)-2,3,4,5-Tetra-*O*-acetyl-1-deoxy-1-*S*-ethyl-1-thio-1-(thymine-1-yl)-aldehydo-*D*-arabinose aldehydrol (**13**).

The fractions from the previously described column containing the slower-moving product (*R*_f 0.40; 2:1 EtOAc–hexane) were combined and the solvent was removed to yield 0.64 g of a clear syrup, which failed to crystallize. Further purification on a column (2.0×40 cm) of silica gel yielded 0.54 g (11%) of **13** as a colorless syrup; [α]_D²⁵ –26.7 (CHCl₃); *R*_f 0.40 (2:1 EtOAc–hexane); EIMS: *m/z* 488 [M]. Anal. Calcd for C₂₀H₂₈N₂O₁₀S·0.5H₂O: C, 48.27; H, 5.89; N, 5.63; S, 6.44. Found: C, 48.54; H, 5.65; N, 5.78; S, 6.18. ¹H NMR and ¹³C

NMR chemical shifts, and proton–proton coupling constants are given in Tables 1, 3, and 4, respectively.

3.5. 1-(2,3,4,5-Tetra-*O*-acetyl-1-deoxy-*D*-arabinitol-1-yl)-thymine (**17**)

To a 100-mL round-bottom flask fitted with a magnetic stirring device was added 0.36 g (0.74 mmol) of compounds **9** + **13** (*R,S* mixture), followed by 25 mL of freshly distilled toluene. To the solution was added 0.85 g (4.0 equiv, 0.80 mL) of Bu₃SnH and 0.02 g of azobisisobutanonitrile (AIBN). The flask was flushed with dry N₂ and maintained under N₂. The mixture was heated to boiling (110 °C) under reflux for 8 h, at which time TLC showed the absence of starting material and the appearance of a single, more-slowly moving spot detectable with both UV absorbance and H₂SO₄ charring. The flask was allowed to cool and the solvent removed under vacuum. The clear syrup was dissolved in 25 mL of *N,N*-dimethylformamide (DMF) and the solution washed three times with 5 mL portions of *n*-hexane. The clear syrup was applied to a column (2.0×40 cm) of silica gel that was eluted with 2:1 EtOAc–hexane as eluent. Fractions containing product **17** were combined to yield 0.30 g (94%) of **12** as a colorless syrup; [α]_D²⁵ +45.9 (CHCl₃); *R*_f 0.17 (2:1 EtOAc–hexane); λ _{max} 272 nm; EIMS: *m/z* 428 [M]. Anal. Calcd for C₁₈H₂₄N₂O₁₀: C, 50.47; H, 5.66; N, 6.54. Found: C, 50.18; H, 5.80; N, 6.31. ¹H NMR and ¹³C NMR chemical shifts, and proton–proton coupling constants are given in Tables 2–4, respectively.

3.6. 1-(1-Deoxy-*D*-arabinitol-1-yl)thymine (**21**)

To a magnetically stirred solution of **17** (2.10 g, 4.90 mmol) in 100 mL of anhydrous MeOH was added a catalytic amount (~0.006 g) of freshly crushed Na. The flask was immediately sealed and the contents were stirred overnight. The basic reaction mixture was then neutralized using cation-exchange resin (Amberlite IR-120, H⁺ form) and the solvent removed under diminished pressure. Addition of pure EtOH yielded 1.10 g (86%) of **21** as small white crystals; mp 230–234 °C (dec), [α]_D²⁵ +38.1 (H₂O); *R*_f 0.53 (1:2 toluene–MeOH). Anal. Calcd for C₁₀H₁₆N₂O₆·0.5H₂O: C, 44.60; H, 6.38; N, 10.40. Found: C, 44.79; H, 6.08; N, 10.23. ¹H NMR and ¹³C NMR chemical shifts, and proton–proton coupling constants are given in Tables 2–4, respectively.

3.7. Preparation of 2,3,4,5-tetra-*O*-acetyl-1-bromo-1-deoxy-1-*S*-ethyl-1-thio-aldehydo-*D*-lyxose aldehydrol (**6**)²

2,3,4,5-Tetra-*O*-acetyl-*D*-lyxose diethyl dithioacetal²³ (**2**, 2.15 g, 5.06 mmol) was treated with Br₂ and the reaction

processed as described for compound **5** to yield **6** as a pale-yellow syrup; R_f 0.44 (3:1 toluene–MeOH), which was used without delay in the next step.

3.8. (1*R,S*)-2,3,4,5-Tetra-*O*-acetyl-1-deoxy-1-*S*-ethyl-1-thio-1-(thymine-1-yl)-aldehydo-*D*-lyxose aldehydrol (**10** and **14**)

Compound **6** (4.72 g, 10.1 mmol) and 2.74 g (1.0 equiv) of 2,4-bis(trimethylsilyl)thymine in 20 mL of dry toluene were allowed to react and the products isolated as described for compounds **9** and **13**, to yield 3.60 g (73%) of yellow syrup containing two major products detectable by both UV absorbance and H₂SO₄ charring. Purification on a column of silica gel afforded 2.71 g of the diastereomers **10** and **14**, as a white foam; yield 54.7%. Analysis by GLC–MS indicated two products with identical mass spectra and retention times of 24.4 and 24.7 min, interpreted as the diastereomeric products **10** and **14** in the ratio of 1.0:1.2.

3.8.1. (1*S*)-2,3,4,5-Tetra-*O*-acetyl-1-deoxy-1-*S*-ethyl-1-thio-1-(thymine-1-yl)-aldehydo-*D*-lyxose aldehydrol (**10**).

The aforementioned foam (2.71 g) was dissolved in a minimal amount of EtOAc and applied to a column (4.0 cm×60 cm) of silica gel (200 g). The column was eluted with 2:1 EtOAc–hexane to separate the products from the reaction mixture. Concentration of the fractions having R_f 0.44 afforded **10** as a white foam; yield 1.15 g (23%); $[\alpha]_D^{25}$ –59.0 (CHCl₃); R_f 0.44 (2:1 EtOAc–hexane); EIMS: m/z 488 [M]. Anal. Calcd for C₂₀H₂₈N₂O₁₀S·0.5H₂O: C, 48.27; H, 5.89; N, 5.63; S, 6.44. Found: C, 48.32; H, 5.71; N, 5.54; S, 6.36. ¹H NMR and ¹³C NMR chemical shifts, and proton–proton coupling constants are given in Tables 1, 3, and 4, respectively.

3.8.2. (1*R*)-2,3,4,5-Tetra-*O*-acetyl-1-deoxy-1-*S*-ethyl-1-thio-1-(thymine-1-yl)-aldehydo-*D*-lyxose aldehydrol (**14**).

The fractions from the previously described column containing the slower-moving product (R_f) 0.40; 2:1 EtOAc–hexane) were combined and the solvent removed to yield 1.48 g of a clear syrup, which failed to crystallize. Further purification on a column (2.0×40 cm) of silica gel yielded 1.38 g (28%) of **14** as a colorless syrup; $[\alpha]_D^{25}$ +72.0 (CHCl₃); R_f 0.40 (2:1 EtOAc–hexane); EIMS: m/z 488 [M]. Anal. Calcd for C₂₀H₂₈N₂O₁₀S·1H₂O: C, 47.41; H, 5.98; N, 5.53; S, 6.33. Found: C, 47.54; H, 5.72; N, 5.54; S, 6.27. ¹H NMR and ¹³C NMR chemical shifts, and proton–proton coupling constants are given in Tables 1, 3, and 4, respectively.

3.9. 1-(2,3,4,5-Tetra-*O*-acetyl-1-deoxy-*D*-lyxitol-1-yl)-thymine (**18**)

Treatment of compounds **10** + **14** (*R,S* mixture, 2.10 g, 4.30 mmol) with Bu₃SnH and AIBN as de-

scribed for **17** yielded 1.50 g (81.5%) of **18** as a colorless syrup; $[\alpha]_D^{25}$ +60.3 (CHCl₃); R_f 0.18 (2:1 EtOAc–hexane); λ_{max} 276 nm (log ϵ 3.87); EIMS: m/z 428 [M]. Anal. Calcd for C₁₈H₂₄N₂O₁₀·0.5H₂O: C, 49.43; H, 5.77; N, 6.41. Found: C, 49.68; H, 5.81; N, 6.47. ¹H NMR and ¹³C NMR chemical shifts, and proton–proton coupling constants are given in Tables 2–4, respectively.

3.10. 1-(1-Deoxy-*D*-lyxitol-1-yl)thymine (**22**)

Catalytic deesterification of **18** (1.40 g, 3.27 mmol) as described for compound **21** yielded 0.79 g (93%) of **22** as small white crystals; mp 220.1–222.3 °C (dec), $[\alpha]_D^{25}$ +45.8 (H₂O); R_f 0.49 (1:2 toluene–MeOH). Anal. Calcd for C₁₀H₁₆N₂O₆·0.5H₂O: C, 44.60; H, 6.38; N, 10.40. Found: C, 44.57; H, 6.44; N, 10.36. ¹H NMR and ¹³C NMR chemical shifts, and proton–proton coupling constants are given in Tables 2–4, respectively.

3.11. Preparation of 2,3,4,5-tetra-*O*-acetyl-1-bromo-1-deoxy-1-*S*-ethyl-1-thio-*D*-ribose aldehydrol (**7**)²

2,3,4,5-Tetra-*O*-acetyl-*D*-ribose diethyl dithioacetal²³ (**3**, 2.15 g, 5.06 mmol) was treated with Br₂ and the reaction processed as described for compound **5** to yield **7** as a pale-yellow syrup; R_f 0.34 (3:1 toluene–MeOH), which was used without delay in the next step.

3.12. (1*R,S*)-2,3,4,5-Tetra-*O*-acetyl-1-deoxy-1-*S*-ethyl-1-thio-1-(thymine-1-yl)-aldehydo-*D*-ribose aldehydrol (**11** and **15**)

Compound **7** (4.72 g, 10.1 mmol) and 2.74 g (1.0 equiv) of 2,4-bis(trimethylsilyl)thymine (**9**) in 20 mL of dry toluene were allowed to react and the products isolated as described for compounds **9** and **13**. Evaporation of the solvent yielded 3.75 g of yellow syrup containing two major products detectable by both UV absorbance and H₂SO₄ charring. Purification on a column of silica gel afforded 3.12 g of the diastereomers **11** and **15**, as a white foam; yield 63%. Analysis by GC–MS indicated two products with identical mass spectra and retention times of 24.0 and 24.3, interpreted as the diastereomeric products **11** and **15** in the ratio of 1.0:3.1.

3.12.1. (1*R*)-2,3,4,5-Tetra-*O*-acetyl-1-deoxy-1-*S*-ethyl-1-thio-1-(thymine-1-yl)-aldehydo-*D*-ribose aldehydrol (**11**).

The aforementioned foam (3.12 g) was dissolved in a minimal amount of EtOAc and applied to a column (4.0 cm × 60 cm) of silica gel (200 g). The column was eluted with 2:1 EtOAc–hexane to separate the products from the reaction mixture. Concentration of the fractions having R_f 0.48 afforded **11** as a white foam that crystallized from pure EtOH; yield 0.75 g (15%); mp 126.0 °C,

$[\alpha]_{\text{D}}^{25} +45.6$ (CHCl_3); R_{f} 0.48 (2:1 EtOAc–hexane); EIMS: m/z 488 [M]. Anal. Calcd for $\text{C}_{20}\text{H}_{28}\text{N}_2\text{O}_{10}\text{S}\cdot 0.5\text{H}_2\text{O}$: C, 48.27; H, 5.89; N, 5.63; S, 6.44. Found: C, 48.11; H, 5.89; N, 5.55; S, 6.12. ^1H NMR and ^{13}C NMR chemical shifts, and proton–proton coupling constants are given in Tables 1, 3, and 4, respectively.

3.12.2. (1S)-2,3,4,5-Tetra-O-acetyl-1-deoxy-1-S-ethyl-1-thio-1-(thymine-1-yl)-aldehydo-D-ribose aldehydrol (15).

The fractions from the previously described column containing the slower-moving product (R_{f} 0.40; 2:1 EtOAc–hexane) were combined and the solvent was removed to yield 2.20 g of a clear syrup, which failed to crystallize. Further purification on a column (2.0×40 cm) of silica gel yielded 2.14 g (43.4%) of **15** as a colorless syrup; $[\alpha]_{\text{D}}^{25} -11.0$ (CHCl_3); R_{f} 0.46 (2:1 EtOAc–hexane); EIMS: m/z 488 [M]. Anal. Calcd for $\text{C}_{20}\text{H}_{28}\text{N}_2\text{O}_{10}\text{S}\cdot 0.5\text{H}_2\text{O}$: C, 48.27; H, 5.89; N, 5.63; S, 6.44. Found: C, 48.45; H, 5.90; N, 5.49; S, 6.16. ^1H NMR and ^{13}C NMR chemical shifts, and proton–proton coupling constants are given in Tables 1, 3, and 4, respectively.

3.13. 1-(2,3,4,5-Tetra-O-acetyl-1-deoxy-D-ribitol-1-yl)-thymine (19)

Treatment of compounds **11** + **15** (R,S mixture, 0.36 g, 1.0 mmol) with Bu_3SnH and AIBN as described for **17** yielded 0.30 g (93%) of **19** as a colorless syrup; $[\alpha]_{\text{D}}^{25} -41.0$ (CHCl_3); R_{f} 0.17 (2:1 EtOAc–hexane); λ_{max} 274 nm; EIMS: m/z 428 [M]. Anal. Calcd for $\text{C}_{18}\text{H}_{24}\text{N}_2\text{O}_{10}$: C, 50.47; H, 5.66; N, 6.54. Found: C, 50.28; H, 5.90; N, 6.20. ^1H NMR and ^{13}C NMR chemical shifts, and proton–proton coupling constants are given in Tables 2–4, respectively.

3.14. 1-(1-Deoxy-D-ribitol-1-yl)thymine (23)

Catalytic deesterification of **19** (1.70 g, 3.97 mmol) as described for compound **21** yielded 1.0 g (97%) of **23** as a white solid; mp 202–205 °C (dec), $[\alpha]_{\text{D}}^{25} -38.6$ (H_2O); R_{f} 0.48 (1:2 toluene–MeOH). Anal. Calcd for $\text{C}_{10}\text{H}_{16}\text{N}_2\text{O}_6$: C, 46.14; H, 6.21; N, 10.77. Found: C, 45.84; H, 6.34; N, 10.52. ^1H NMR and ^{13}C NMR chemical shifts, and proton–proton coupling constants are given in Tables 2–4, respectively.

3.15. Preparation of 2,3,4,5-tetra-O-acetyl-1-bromo-1-deoxy-1-S-ethyl-1-thio-aldehydo-D-xylose aldehydrol (8)²

2,3,4,5-Tetra-O-acetyl-D-xylose diethyl dithioacetal²³ (**4**, 2.15 g, 5.06 mmol) was treated with Br_2 and the reaction processed as described for compound **5** to yield **8** as a pale-yellow syrup; R_{f} 0.31 (3:1 toluene–MeOH), which was used without delay in the following step.

3.16. (1R,S)-2,3,4,5-Tetra-O-acetyl-1-deoxy-1-S-ethyl-1-thio-1-(thymine-1-yl)-aldehydo-D-xylose aldehydrol (12 and 16)

Compound **8** (4.72 g, 10.1 mmol) and 2.74 g (1.0 equiv) of 2,4-bis(trimethylsilyl)thymine in 20 mL of dry toluene were allowed to react and the products isolated as described for compounds **9** and **13** to yield 4.22 g (86%) of yellow syrup containing two major products detectable by both UV absorbance and H_2SO_4 charring. Purification on a column of silica gel afforded 3.22 g of the diastereomers **12** and **16**, as a white foam; yield 65%. GLC–MS analysis indicated two products with identical mass spectra and retention times of 24.3 and 24.8, interpreted as the diastereomeric products **12** and **16** in the ratio of 2.2:1.0.

3.16.1. (1S)-2,3,4,5-Tetra-O-acetyl-1-deoxy-1-S-ethyl-1-thio-1-(thymine-1-yl)-aldehydo-D-xylose aldehydrol (16).

The aforementioned foam (3.22 g) was dissolved in a minimal amount of EtOAc and applied to a column (3.5×60 cm) of silica gel (200 g). The column was eluted with 2:1 EtOAc–hexane to separate the products from the reaction mixture. Concentration of the fractions having R_{f} 0.50 afforded **16** as a white foam that crystallized from pure EtOH; yield 2.07 g (42%); mp 124.0–125.0 °C, $[\alpha]_{\text{D}}^{25} -116$ (CHCl_3); R_{f} 0.50 (2:1 EtOAc–hexane); EIMS: m/z 488 [M]. Anal. Calcd for $\text{C}_{20}\text{H}_{28}\text{N}_2\text{O}_{10}\text{S}\cdot 0.5\text{H}_2\text{O}$: C, 48.27; H, 5.89; N, 5.63; S, 6.44. Found: C, 48.34; H, 5.70; N, 5.58; S, 6.19. ^1H NMR and ^{13}C NMR chemical shifts, and proton–proton coupling constants are given in Tables 1, 3, and 4, respectively.

3.16.2. (1R)-2,3,4,5-Tetra-O-acetyl-1-deoxy-1-S-ethyl-1-thio-1-(thymine-1-yl)-aldehydo-D-xylose aldehydrol (12).

The fractions from the previously described column containing the slower-moving product (R_{f} 0.43; 2:1 EtOAc–hexane) were combined and the solvent removed to yield 1.18 g of a clear syrup, which failed to crystallize. Further purification on a column (2.0×40 cm) of silica gel yielded 1.10 g (22%) of **12** as a colorless syrup; $[\alpha]_{\text{D}}^{25} +43.4$ (CHCl_3); R_{f} 0.43 (2:1 EtOAc–hexane); EIMS: m/z 488 [M]. Anal. Calcd for $\text{C}_{20}\text{H}_{28}\text{N}_2\text{O}_{10}\text{S}\cdot 0.5\text{H}_2\text{O}$: C, 48.27; H, 5.89; N, 5.63; S, 6.44. Found: C, 48.27; H, 5.76; N, 5.69; S, 6.19. ^1H NMR and ^{13}C NMR chemical shifts, and proton–proton coupling constants are given in Tables 1, 3, and 4, respectively.

3.17. 1-(2,3,4,5-Tetra-O-acetyl-1-deoxy-D-xylitol-1-yl)-thymine (20)

Treatment of compounds **12**+**16** (R,S mixture, 3.20 g, 6.55 mmol) with Bu_3SnH and AIBN as described for **17** yielded 2.60 g (92.5%) of **20** as a colorless syrup;

$[\alpha]_{\text{D}}^{25} +45.9$ (CHCl₃); R_{f} 0.17 (2:1 EtOAc–hexane); λ_{max} 274 nm; EIMS: m/z 428 [M]. Anal. Calcd for C₁₈H₂₄N₂O₁₀·1H₂O: C, 48.45; H, 5.89; N, 6.28. Found: C, 48.62; H, 5.63; N, 6.21. ¹H NMR and ¹³C NMR chemical shifts, and proton–proton coupling constants are given in Tables 2–4, respectively.

3.18. 1-(1-Deoxy-D-xylitol-1-yl)thymine (24)

Catalytic deesterification of **20** (2.30 g, 5.37 mmol) as described for compound **21** yielded 1.30 g (93%) of **24** as a white powder; mp 117.0–120.2 °C (dec), $[\alpha]_{\text{D}}^{25} -37.4$ (H₂O); R_{f} 0.64 (1:2 toluene–MeOH). Anal. Calcd for C₁₀H₁₆N₂O₆·0.5H₂O: C, 44.60; H, 6.38; N, 10.40. Found: C, 44.55; H, 6.37; N, 10.49. ¹H NMR and ¹³C NMR chemical shifts, and proton–proton coupling constants, are given in Tables 2–4, respectively.

3.19. Toxicological effects of 1-(1-deoxy-D-pentitol-1-yl)-thymines (21–24) versus *Cucumis sativus* and *Nicotiana tabacum*

A 100-ppm aqueous solution of each separate 1-(1-deoxy-D-pentitol-1-yl)thymine was applied to cucumber (*C. sativus*, 14 days following germination) and tobacco plants (*N. tabacum*, 20 days following germination) using the previously described air-brush technique.²⁴ Each test group comprised 4 cucumber and 3 tobacco plants, and received 10.0 mL of test solution. A group of 4 cucumber plants and 3 tobacco plants treated in the same manner using distilled water instead of the 1-(1-deoxy-D-arabinitol-1-yl)thymine solution was established as the control group. Following the application, the plants remained in the application hood for 1 h and were then moved to a climate-controlled greenhouse (25 °C) for 24 h. After the incubation period, the poor condition of the plants indicated that they could not withstand the concentration of the applied test solution. Appropriate dilutions were performed to achieve test solution concentrations of 10.0, 25.0, and 50.0 ppm. To test groups identical to those just described, 10.0 mL of each diluted solution was applied and the plants were incubated for 24 h in the greenhouse. Following the incubation period, the plants were studied for signs of stress resulting from the chemical treatment. As no significant differences were noted in comparison with the control groups, the procedure of viral infection was undertaken.

3.20. Resistance of *C. sativus* treated with 1-(1-deoxy-D-pentitol-1-yl)thymines (21–24) toward cucumber green mottle mosaic virus (CGMMV) infection

A solution of CGMMV was prepared for inoculation in the following manner: a sample of infected cucumber plant leaves (1.0 g) was pulverized using a mortar and pestle. A phosphate-buffer solution (0.1 M, 200.0 mL,

pH 7) was added to the mixture to facilitate the homogenization process. The mixture was filtered through gauze to yield a green solution of the virus. To this solution was added 2.0 g of carborundum abrasive (C600 mesh). Finally the solution was applied to the cucumber plant test-subjects via the air-brush technique. The plants were returned to the climate-controlled greenhouse and monitored daily for signs of infection (leaf discolorations, leaf distortions, leaf spots, and/or stem symptoms).

3.21. Resistance of *N. tabacum* treated with 1-(1-deoxy-D-pentitol-1-yl)thymines (21–24) toward tobacco mosaic virus (TMV) infection

A solution of TMV was prepared for inoculation in the following manner: a sample of infected tobacco plant leaves (2.0 g) was pulverized using a mortar and pestle. A phosphate-buffer solution (0.1 M, 200.0 mL, pH 7) was added to the mixture to facilitate the homogenization process. The mixture was filtered through gauze to yield a green solution of the virus. To this solution was added 2.0 g of carborundum abrasive (C600 mesh). Finally the solution was applied to the tobacco plant test-subjects via the air-brush technique. The plants were returned to the climate-controlled greenhouse and monitored daily for signs of infection (leaf discolorations, leaf distortions, leaf spots including mosaics, and/or stem symptoms).

3.22. Toxicological effects of 1-(1-deoxy-D-pentitol-1-yl)-thymines (21–24) versus potted rice plants (*v. Koshihikari*)

Aqueous solutions of each 1-(1-deoxy-D-pentitol-1-yl)thymine were prepared at 10, 50, and 100 ppm concentrations. Using the previously described air-brush technique, 20 mL of each test solution was applied to test groups consisting of four rice plants each. The tested plants were all selected at the 3.5–4 leaf stage. An additional group of four potted rice plants treated in a similar manner using distilled water instead of the 1-(1-deoxy-D-pentitol-1-yl)thymine solution was established as the control group. Following the application, the plants remained in the application hood for 1 h and were then moved to a climate-controlled greenhouse (25 °C) for 24 h. Following the incubation period, the plants were studied for signs of stress resulting from the chemical treatment. As no significant differences were noted in comparison with the control group, the procedure of fungal infection was undertaken.

3.23. Resistance of potted rice plants (*v. Koshihikari*) treated with 1-(1-deoxy-D-pentitol-1-yl)thymines (21–24) toward *Pyricularia oryzae*, Hoku 1 race 007 infection

A solution of the rice blast fungus, *P. oryzae*, was grown on oatmeal agar medium for 2 weeks at 28 °C in the

absence of light. The plates were then irradiated with a UV source to induce conidiation. Abundant conidia were produced on the surface within 3 days. A suspension of the conidia was prepared by pouring a small amount of distilled water onto the plate and rubbing the media with a sterilized brush. The conidia suspension was filtered and the concentration adjusted to approximately 10^7 /mL using distilled water. Finally the solution was applied to the previously treated potted rice plants in a partially enclosed chamber using the air-brush technique. The chamber was maintained at a high level of humidity, a temperature of 24 °C, and completely isolated from exterior light sources. Following the 24-h incubation period in the dark, the plants were returned to the climate-controlled greenhouse and monitored daily for signs of infection (leaf discolorations, leaf distortions, leaf spots, and/or stem symptoms).

Acknowledgments

S.M.V. thanks the US National Science Foundation for support for a Summer Program in Japan and Dr. Isamu Yamaguchi and his laboratory for the opportunity provided to perform the plant toxicological studies reported here.

References

1. Wolfrom, M. L.; Bhat, H. B.; McWain, P.; Horton, D. *Carbohydr. Res.* **1972**, *23*, 289–295; Horton, D.; Kokrady, S. S. *Carbohydr. Res.* **1972**, *24*, 333–341.
2. Baker, D. C.; Horton, D. *Carbohydr. Res.* **1979**, *69*, 117–134.
3. Horton, D.; Markovs, R. A. *Carbohydr. Res.* **1980**, *80*, 263–275.
4. Horton, D.; Kokrady, S. S. *Carbohydr. Res.* **1980**, *80*, 364–374.
5. Horton, D.; Baker, D. C.; Kokrady, S. S. *Ann. NY Acad. Sci.* **1975**, *225*, 131–150.
6. Elion, G. B.; Furman, P. A.; Fyfe, J. A.; de Miranda, P.; Beauchamp, L.; Schaeffer, H. J. *Proc. Natl. Acad. Sci. U.S.A.* **1977**, *74*, 5716–5720.
7. Schaeffer, H. J.; Beauchamp, L.; de Miranda, P.; Elion, G. B.; Bauer, D. J.; Collins, P. *Nature* **1978**, *272*, 583–585.
8. Gauthier, B. *Ann. Pharm. Fr.* **1954**, *12*, 281–285.
9. Weygand, F.; Ziemann, H.; Bestmann, H. J. *Chem. Ber.* **1958**, *91*, 2534–2537.
10. Nishimura, T.; Iwai, I. *Chem. Pharm. Bull. (Tokyo)* **1964**, *12*, 357–361.
11. Nishimura, T.; Shimizu, B.; Iwai, I. *Chem. Pharm. Bull. (Tokyo)* **1964**, *12*, 1470–1472.
12. Nishimura, T.; Iwai, I. *Chem. Pharm. Bull. (Tokyo)* **1964**, *12*, 352–356.
13. Vejcik, S. M. Ph.D. Dissertation, American University, 2002.
14. Shugar, D.; Fox, J. J. *Biochem. Biophys. Acta* **1952**, *9*, 199–218.
15. Kokrady, S. S. Ph.D. Dissertation, Ohio State University, 1972.
16. Horton, D.; Thomas, S.; Gallucci, J. *Carbohydr. Res.* **2006**, *341*, 2211–2218.
17. El Khadem, H. S. *Carbohydr. Res.* **1977**, *59*, 11–18.
18. Blieszner, K. C.; Horton, D.; Markovs, R. A. *Carbohydr. Res.* **1980**, *80*, 241–262.
19. Horton, D.; Wander, J. D. *Carbohydr. Res.* **1969**, *10*, 279–288; Horton, D.; Wander, J. D. *Carbohydr. Res.* **1970**, *13*, 33–47; Horton, D.; Wander, J. D. *Carbohydr. Res.* **1970**, *15*, 271–284.
20. Horton, D.; Durette, P. L.; Wander, J. D. *Ann. NY Acad. Sci.* **1973**, *222*, 884–914.
21. Horton, D.; Wander, J. D. *J. Org. Chem.* **1974**, *39*, 1859–1863.
22. Muesser, M.; Defaye, J. D.; Horton, D. *J. Org. Chem.* **1978**, *43*, 3053–3055.
23. Horton, D.; Wander, J. D. *Adv. Carbohydr. Chem. Biochem.* **1976**, *32*, 15–123.
24. Huang, K. T.; Matsuzawa, Y.; Misato, T. *Phytopathol. Soc. Jpn.* **1974**, *40*, 1–5.